https://doi.org/10.22226/2410-3535-2020-2-164-169 PACS: 61.66.Fn, 62.20.-x

The effect of reduced graphene oxide (rGO) and thermally exfoliated graphite (TEFG) on the mechanical properties of "nickel-graphene" composites

O. Yu. Kurapova[1], I. V. Smirnov[1], E. N. Solovyeva[2], I. Yu. Archakov[†,2,3], V. G. Konakov[1,2]

[†]Ivan.Archakov@gmail.com

[1]Saint Petersburg State University, 7/9 Universitetskaya emb., St. Petersburg, 199034, Russia
[2]Peter the Great Saint Petersburg Polytechnic University, 29 Polytechnicheskaya St., St. Petersburg, 195251, Russia
[3]Institute of Problems of Mechanical Engineering RAS, 61 Bolshoy Av. VO, St. Petersburg, 199178, Russia

Nickel matrix composites are important materials for various engineering applications. The present paper describes the fabrication of bulk graphene-nickel (Gr-Ni) and reduced graphene oxide-nickel (rGO-Ni) composites by powder metallurgy technique using various graphene sources, namely, thermally exfoliated graphite (TEFG) and reduced graphene oxide (rGO) and the investigation of the mechanical properties of the composites. Homogeneous distribution of graphene derivatives in the composite matrices was confirmed for all compositions by XRD and Raman spectroscopy. It was proved that different Gr sources in the initial powder mixtures result in some different graphene derivatives type in the composites produced. Nevertheless, scanning electron microscopy data demonstrated that the microstructure of the samples produced using the different graphene sources is rather similar. It was shown that the mechanical properties of the composites are very sensitive to the type of graphene derivative chosen at low additive contents. TEFG addition results in the decreased values of tensile strength, ductility, and elongation for all compositions. It was shown that 0.1 wt.% of rGO addition resulted in the 34% elongation-to-failure increase with no change in the UTS value of composite. The 0.1 wt.% rGO-Ni composite showed the increased elongation and the tensile strength value comparable to pure nickel specimen. Fractography tests revealed the difference in the mechanical behaviour of rGO-Ni and Gr-Ni composites.

Keywords: nickel matrix composite, graphene, reduced graphene oxide, tensile strength, hardness.

УДК: 669-1

Влияние восстановленного оксида графена (rGO) и терморасширенного графита (TEFG) на механические свойства никель-графеновых композитов

Курапова О. Ю.[1], Смирнов И. В.[1], Соловьева Е. Н.[2], Арчаков И. Ю.[†,2,3], Конаков В. Г.[1,2]

[1]Санкт-Петербургский государственный университет, Университетская наб., 7/9, С.-Петербург, 199034, Россия
[2]Санкт-Петербургский политехнический университет Петра Великого,
ул. Политехническая, 29, С.-Петербург, 195251, Россия
[3]Институт проблем машиноведения РАН, Большой пр. ВО, 61, С.-Петербург, 199178, Россия

Композиты с никелевой матрицей являются важными материалами для различных технических применений. В настоящей статье описывается изготовление объемных графен-никелевых (Gr-Ni) композитов на основе никеля с восстановленным оксидом графена (rGO-Ni) методом порошковой металлургии с использованием различных источников графена, а именно терморасширенного графита (TEFG) и восстановленного оксида графена (rGO) и исследование механических свойств композитов. Однородное распределение производных графена в никелевой матрице было подтверждено для всех составов методами рентгеновской и рамановской спектроскопии. Было доказано, что различные источники Gr в исходных порошковых смесях приводят к некоторому различному типу производных графена в полученных композитах. Тем не менее данные сканирующей электронной микроскопии

показали, что микроструктура образцов, полученных с использованием различных источников графена, довольно схожа. Было показано, что механические свойства композитов очень чувствительны к типу производного графена, выбранного при низком содержании добавки. Добавление TEFG приводит к снижению значений прочности на растяжение, пластичности и удлинения для всех композиций. Было показано, что добавление 0.1 мас.% rGO приводило к увеличению удлинения до разрушения на 34% без изменения значения предела прочности для композита. Композит rGO-Ni с концентрацией 0.1 мас.% показал увеличенное удлинение и предел прочности на разрыв, сопоставимый с образцом чистого никеля. Фрактографические тесты выявили разницу в механическом поведении композитов rGO-Ni и Gr-Ni.

Ключевые слова: композит с никелевой матрицей, графен, восстановленный оксид графена, предел прочности, твердость.

1. Introduction

Nickel-matrix composites are in high demand for automobile and aerospace industries due to high strength, lighter weight, relatively low thermal expansion and corrosion. Recently, it has been shown [1–3] that the addition of graphene (Gr) as a modifying additive is preferable over other carbon-based fillers: carbon nanotubes (CNTs), carbon fibers, etc. Great mechanical characteristics of graphene-nickel (Gr-Ni) composites are attributed to the homogeneous incorporation of Gr into a nickel matrix and, unlike copper and aluminum, a possibility of strong bonding between graphene and Ni [3]. Analysis of the data reported in modern literature shows [4–6] that the achievement of homogeneous distribution and sufficient bonding between graphene and metal matrix is governed by following key issues: (i) a type of Gr-containing additive and (ii) the synthesis technique chosen. It should be noted that graphene in its single-layered form is rarely used for metal matrix composite synthesis due to the instability caused by free surface energy excess of the material. That induces severe graphene agglomeration and its stacking to multilayered flakes [7]. As an alternative to monolayer Gr, graphene derivatives are used to produce Gr-modified composites: graphene nanoplatelets, graphene oxide (GrO), and reduced graphene oxide (rGO) should be noted here as they possess the defect structure as well as high level of oxygen containing groups that prevent their agglomeration. As mentioned in [8], the oxygen-mediated bonding between residual rGO groups and nickel atoms can result in the enhanced interfacial bonding in rGO-Ni composites.

Several processing approaches were proposed for effective dispersing of Gr derivatives in a Ni matrix. It should be noted that the major part of the publications is devoted to the electrochemical deposition [5,9–11], which allows to obtain a required uniformity of the graphene distribution; however, this approach allows only films/coatings fabrication. According to [9], the elastic modulus of the composite electrochemically deposited from the solution containing 0.05 g Gr per 1L was 1.7 times higher than that for pure Ni deposited under the same conditions (240 GPa), while the hardness of the composite layer exceeded the hardness of pure Ni layer by 1.2 times (4.6 GPa). Kim et al. fabricated Gr-Ni nanolayered composite films by chemical vapor deposition [5]. The films consisted of alternating Ni layers and Gr monolayers with 100-nm repeat layer spacing. Such Gr-Ni composite films demonstrated extremely high mechanical characteristics. The values of flow stress being 5% and plastic strain up to 4 GPa, obtained in the nanopillar tension tests, were reported. In [8], the synthesis of Ni-based composite reinforced by reduced graphene oxide was performed via molecular level mixing with following spark plasma synthesis (SPS) technique. Bulk Ni-1.5 wt.% Gr composites characterized by the 95.2% increased tensile strength and 327.6% increased yield strength and simultaneously retained a 12.1% of elongation were obtained. *In-situ* high-temperature CVD process followed by SPS was suggested in [3] to prepare uniform bulk Ni-Gr composites. The fabrication of bulk Ni-Gr composites by graphene *in-situ* growth in the nickel matrix using the powder metallurgy method was reported in [12].

In all cases authors used both various Gr derivatives and modern techniques which are often rather complicated. So, the particular effects of the manufacturing technique and the graphene reinforcing additive itself still remain fairly unclear. The modified powder metallurgy technique was recently suggested in the works of the authors of the present study; the suggested approach provides the homogeneous Gr distribution in various metal and ceramic matrices [13–15]. No destruction of the Gr structural integrity nor its amorphization were shown to take place during milling, processing, and thermal treatment steps of the production procedure.

Summarizing the above data, one can see that the information on the impacts of the Gr derivative type and manufacturing technique would allow a possibility of novel Gr-Ni composites development. So, the goal of the present work was the study of the Gr source effect (rGO or thermally exfoliated graphite) on the mechanical properties of bulk Gr-Ni composites.

2. Materials and methods

Micron-sized Ni powder (60–80 μm, "Advanced Powder Technologies", Ltd., Russia) was used as a starting material for the composites manufacturing. rGO manufactured by modified Hummers technique [15–17] and commercial TEFG platelets were taken as Gr sources. Sample 1 (the reference one) was produced from pure Ni powder. Primary powder mixtures containing 0.1, 0.2, 0.5, 1.0 wt.% rGO were used to produce Samples 2–5, respectively, and mixtures with 0.1 and 0.5 wt.% of TEFG were used to manufacture Samples 6 and 7, respectively. The prepared powder mixtures were ball milled (Pulverisete-6, 400 rpm for 2 hours 2 min. reverse cycles). Then powders were compacted using cold isostatic pressing (12.5 ton/cm^2, 15 min), the pellets with 25 mm diameter and 9 mm height were manufactured. Then the samples were annealed in a vacuum furnace at 1250°C for 1 hour.

The identification of the Samples phase composition was performed by X-ray diffraction analysis (XRD, SHIMADZU XRD-6000, Cu-K_α at α=1.5406 Å). Raman spectroscopy (SENTERRA, T64000, excitation wave length 526 nm) was used to identify carbon allotropes. Scanning electron microscopy (SEM, Hitachi S-3400N), electron back-scattering diffraction (EBSD, Hitachi S-3400N) were used to analyze the microstructure of specimens (rectangular grid with the step size of 0.5 μm for 23 μsec per one mapping). Vickers microhardness tests (Shimadzu HMV-G21DT) were performed using diamond pyramidal indenter with 0.5 N load applied for 15 seconds (data averaged over 15 tests along the Sample's cross-section). Mechanical properties tests were carried out via uniaxial tensile tests (SHIMADZU AG-50kNX, strain rate of 10^{-3} s^{-1}). The flat dog-bone shaped specimens were cut along the cross-section of the Samples using electrical discharge machine (working part: 6 mm in length, 2 mm in width, 1.3 mm in thickness). The data was averaged over 3 specimens per each Sample. Fractography (Zeiss Auriga Laser) was used to perform failure analysis of the Samples.

3. Results and discussion

Typical Raman spectroscopy results for Samples 2 and 6 manufactured using different Gr sources are shown in Fig. 1, the spectra obtained are generally similar. The position of D band for both Samples is 1350 cm^{-1}, whereas the position of G band depends on the Gr source used. The position of G peak in Sample 2 spectrum is slightly shifted comparing to spectrum obtained for pure rGO (Fig. S1, Supplementary Material) [15] and with the results for rGO-Ni composites obtained by SPS [8]: 1587 cm^{-1} (Sample 2) vs 1575 cm^{-1} for pure rGO and 1580 cm^{-1} for Ni-Gr composites [8,15]. Since G band is due to ordered state of sp^2 carbon lattice, the shift observed, likely, indicates the interaction of rGO with the nickel matrix. The I_D/I_G intensity ratio is ~0.75 – 0.78 for Samples 2 – 5 and ~0.85 for Samples 6 and 7; following [6,8,10], I_D/I_G is <1 indicates that no structural damage of Gr derivative took place.

XRD patterns (Fig. S2, Supplementary Material) show the absence of oxides and carbides in all Samples. Note that the Gr contents in all Samples was below the sensitivity limit of the approach, hence, no direct information on Gr derivatives was obtained.

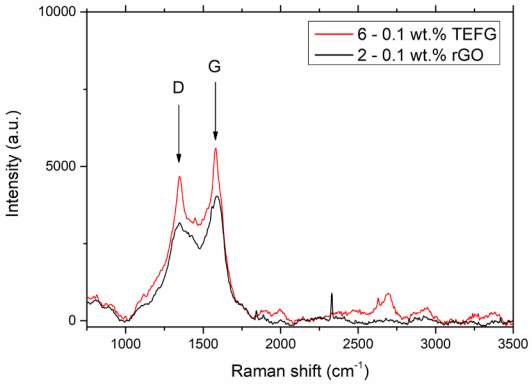

Fig. 1. (Color online) Raman data for Samples 2 and 6 fabricated from powder mixtures with different Gr sources.

SEM images of Samples surface are shown in Fig. 2. Comparing the microstructure of pure Ni Sample and composite Samples 2, 5, and 6, one can see that low (0.1 wt.%) contents of both rGO and TEFG results in slight porosity decrease. Elongated pores along the grain boundaries that present in pure nickel are almost absent in the composites. rGO can be considered as some more effective porosity inhibitor (Fig. 3 b, c) due to the absence of the elongated and interconnected pores. The increase of rGO contents in the initial powder mixture up to 1 wt.% results in microstructural inhomogeneity and severe cracks formation. In parallel with [15,18] two possible mechanisms may cause the cracking: (i) difference of thermal expansion coefficient of graphene and nickel matrix may result in the lattice distortion on the interfaces, voids formation during heating-cooling step; (ii) Gr agglomerates hinder the composite powder compaction thus increasing the distance between Ni powder particles and decreasing powder sintering ability or limiting material matrix flow. Both factors induce pores/voids formation in composite and, thus, the cracking.

The EBSD results obtained for Samples 1 and 4 are shown in Fig. 3. It demonstrates that pure nickel Sample is composed of mostly elongated grains, its microstructure is characterized by moderate porosity. The introduction of 0.5 wt.% rGO results in more homogeneous structure. Slight grain coarsening takes place along with pores size decrease (Fig. S3, Supplementary Material) from ~5 to ~8 μm. In case of pure nickel both coarse and fine grains, likely, present in the structure due to wider particle size distribution in the initial precursor. Grain growth takes place according to the mechanism when coarser grains are formed due to finer grains merging. During milling graphene flakes form a layer on the Ni agglomerates, but not the individual particles [15,18]. So the distribution of agglomerates by size, likely, becomes narrower and slightly coarser grains of similar size are obtained after sintering. In both pure nickel and composite specimen, the amount of high-angle grain boundaries (HAB) is rather low.

The dependence of Vickers microhardness on rGO and TEFG content is shown in Fig. 4. Microhardness values of pure nickel and composites with 0.1 and 0.2 wt.% Gr

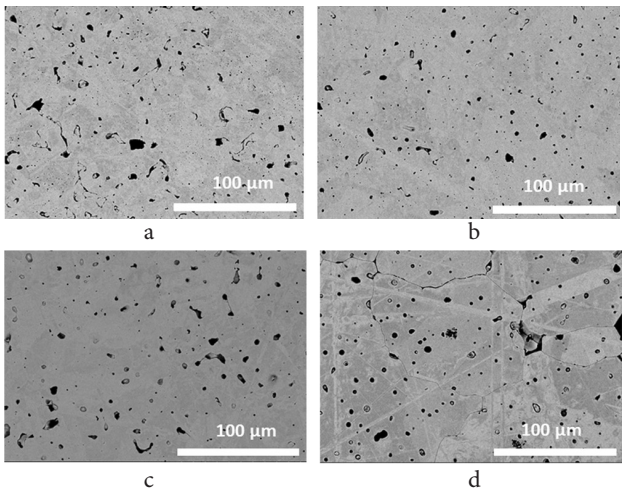

Fig. 2. SEM images in backscattered regime for Samples 1 (pure Ni) (a); 2 (0.1 wt.% rGO) (b); 6 (0.1 wt.% TEFG) (c); 5 (max rGO contents of 1 wt.%) (d).

derivative are close to each other within the experimental error. Remarkably, the Gr source chosen (TEFG, rGO) does not affect the microhardness values and composites 2 and 6, as well as 4 and 7 showed the same microhardness within the measurement error. Microhardness increase takes place with graphene derivative content increase to 0.5 and 1 wt.%. Sample 5 showed the highest hardness of 106.3±10.3 HV. The effect of graphene source is more evident on the mechanical properties of samples. Fig. 5 presents typical stress-strain curves obtained for Samples 1–7, see also Table 1.

As seen from Fig. 5 and Table 1, generally, the incorporation of both rGO and TEFG to Ni matrix results in a gradual decrease of composites tensile strength and ductility. The change of UTS, yield strength and elongation at break of rGO-Ni composites is non-linear. Sample 2 (0.1 wt.% rGO) showed the increased elongation along with the same UTS value as pure nickel which is uncommon for metal matrix composites, while the same TEFG amount does not provide the same effect and lower UTS value is observed. Further increase of rGO and TEFG contents resulted in the decreased mechanical properties. The type of Gr source did not produce obvious difference in UTS, yield strength and elongation values for Samples 4 and 7 (0.5 wt.% Gr). It should be noted that despite the highest Vickers microhardness values, Sample 5 with 1 wt.% rGO contents demonstrated drastically reduced tensile strength.

Note that the obtained data agree with results obtained for Gr-Ni composites produced from Ni nanopowder [13]. In spite of the fact that the use of nanopowders provided much higher UTS and yield strength, the same tendency to UTS decrease at Gr contents increase is observed. Following [5,8], some increase in Sample 2 mechanical properties can be attributed to homogeneously dispersed carbon additive and strong interphase rGO bonding with Ni matrix.

Thus the simultaneous decrease of strength and ductility of the composite materials obtained in the current work can be explained from the position of the agglomeration of rGO and TEFG excess on the grain boundaries of the nickel matrix which leads to the low interphase bonding between graphene derivative and nickel matrix. In case of TEFG additive the agglomeration is due to the presence of graphite which was not completely converted to graphene during ball milling. Such coarse bundles of graphene are not able to effectively transfer stress and efficiently constrain the dislocations propagation across the interface.

The above discussed data agree with the fractography results, see Figs. 6 and 7). The pronounced slip traces on the grain surface, as well as the presence of secondary cracks on

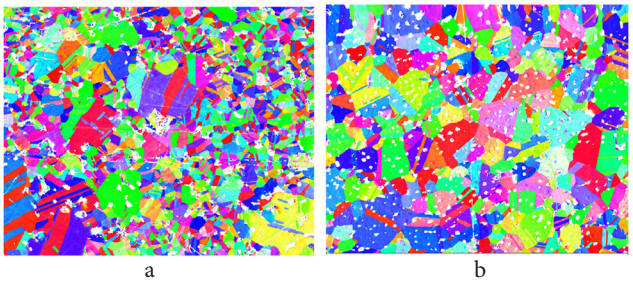

Fig. 3. (Color online) EBSD maps obtained for Sample 1 (a) and 4 (b).

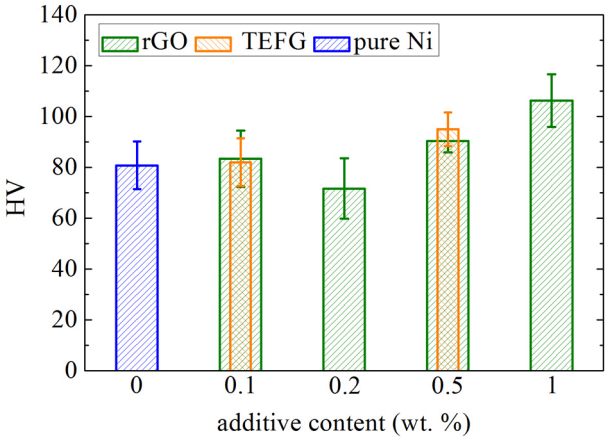

Fig. 4. (Color online) The effect of graphene contents on Vickers microhardness of composites.

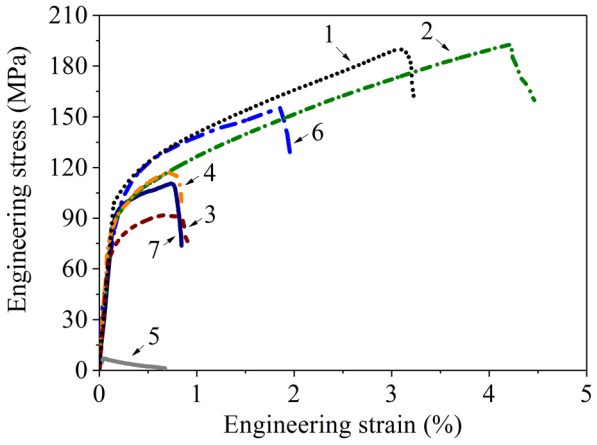

Fig. 5. (Color online) Typical stress-strain curves obtained for Gr-Ni composites.

Table 1. The results of mechanical testing of composites 1–7.

Sample	Ultimate tensile strength [MPa]	Yield limit [MPa]	Elongation [%]
1	174.19±16.63	110.26±2.74	2.91±0.29
2	175.28±35.21	112.55±35.16	3.07±1.39
3	79.89±14.14	52.26±4.56	0.60±0.30
4	109.07±5.99	81.46±12.18	0.69±0.21
5	6.50±0.45	-	1.30±0.96
6	156.62±26.22	119.99±7.33	3.23±1.81
7	106.04±5.09	93.68±1.60	0.59±0.30

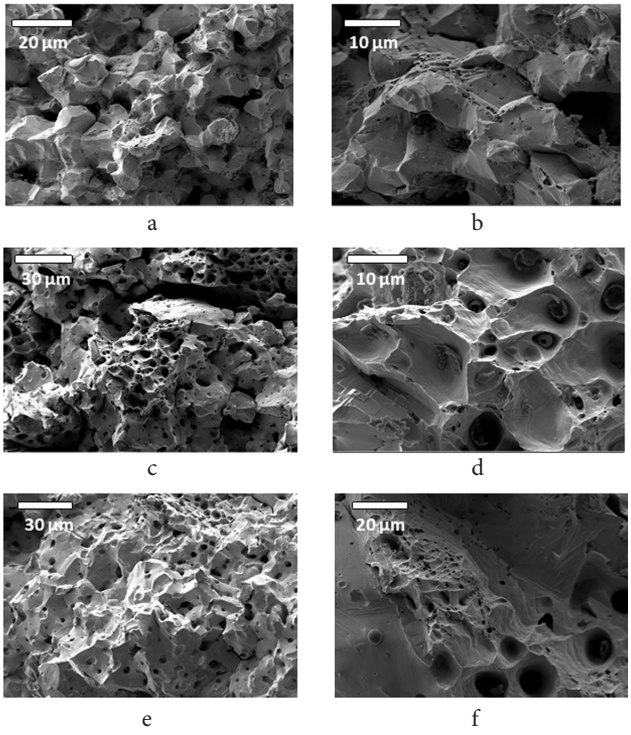

Fig. 6. SEM images of fracture surface of Sample 1 (a and b), Sample 2 (c and d), and Sample 6 (e and f) after the tensile tests.

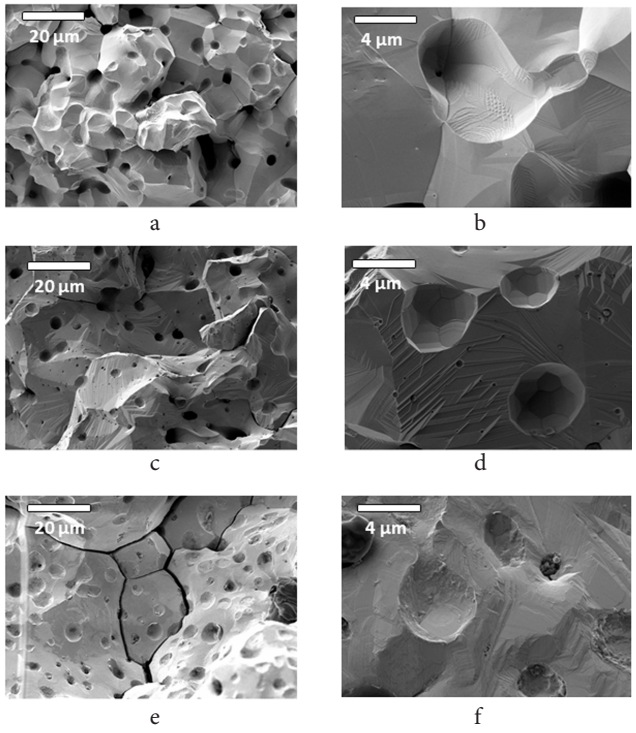

Fig. 7. SEM images of fractured surface of: Sample 3 (a and b), Sample 4 (c and d), Sample 5 (e and f) after the tensile tests.

the grain boundaries and pore craters are common features for all fracture surfaces obtained. A fracture surface of pure nickel (Sample 1) corresponds to mainly intergranular type of fracture along with the presence of secondary cracks and slip bands on the surface of grain boundaries (see Fig. 6 a, b). Besides, the zones of dimple-like fracture with the sizes of 2 – 5 μm are randomly located on the fracture surface. The addition of rGO or TEFG results in more smooth details of relief. The fracture surfaces here can be divided into groups. The first group (see Fig. 6) includes similar surfaces of Samples 2 and 6 (0.1 wt.% rGO and TEFG).The mixed fracture mechanism corresponds to this group. In addition to the smoothened grain boundaries, their fracture surface contains multiple zones of cone dimples with the diameter up to 10 μm.

The second group (see Fig. 7) includes the surfaces of Samples 3 – 5 and 7. The surfaces of Samples 4 and 7 (0.5 wt.% of Gr derivative) are quite similar. They are characterized by the absence of typical dimple-like fracture, but a lot of crater-like features are present here. These surfaces differ just in the degree of smoothing of angle grain boundaries which increase with the increase of graphene derivative content as well as the surface of craters itself.

4. Conclusions

Using XRD, SEM, and Raman spectroscopy, it was shown that obtained graphene-nickel composites possess the homogeneous distribution of rGO and graphene in the nickel matrix. Raman spectroscopy revealed a certain amount of graphite present in Gr-Ni composites obtained using TEFG. It was shown that 0.1 wt.% of rGO addition resulted in the 34% elongation-to-failure increase with no change in the UTS value of composite. The results of mechanical testing indicated the decrease of UTS value of composites and moderate microhardness increase with the increase of rGO and TEFG content. Despite high Vickers microhardness values, composite manufactured from 1 wt.% rGO-Ni powder mixture showed drastically low tensile strength.

Supplementary Material. *The online version of this paper contains supplementary material available free of charge at the journal's Web site (lettersonmaterials.com).*

Acknowledgements. This work was supported by Russian foundation for basic research (RSBF #18-29-19086). Raman spectroscopy data, SEM data of the composites and composites after fractography tests were obtained at the Research park of St. Petersburg State University «Center for Optical and Laser Materials Research», «Center for Geo-Environmental Research and Modeling (GEOMODEL)» and «Interdisciplinary Center for Nanotechnology», respectively. The mechanical testing was performed under support of Ministry of Education and Science of Russian Federation under Grant Zadanie #16.3483.2017/PCh.

References

1. S. C. Tjong. Mater. Sci. Eng. R. 74, 281 (2013). Crossref
2. I. A. Ovidko. Rev. Adv. Mater. Sci. 38, 190 (2014).
3. K. Fu, X. Zhang, C. Shi, E. Liu, F. He, J. Li, N. Zhao, C. He. Mater. Sci. Eng. A. 715, 108 (2018). Crossref
4. K. Chu, C. Jia. Phys. Status Solidi A. 211, 184 (2014). Crossref
5. Y. Kim, J. Lee, M. Yeom, J. Shin, H. Kim, Y. Cui, J. Kysar, J. Hone, Y. Jung, S. Jeon, S. Han. Nature. Commun. 4, 2114 (2013). Crossref

6. T. Borkar, H. Mohseni, J. Hwang, T.W. Scharf, J.S. Tiley, S.H. Hong, R. Banerjee. Journal of Alloys and Compounds. 646, 135 (2015). Crossref
7. A.G. Glukharev, V.G. Konakov. Rev. Adv. Mater. Sci. 56, 124 (2018). Crossref
8. C. Zhao. Applied Physics A. 118, 409 (2015). Crossref
9. Z. Ren, N. Meng, K. Shehzad, Y. Xu, S. Qu, B. Yu, J.K. Luo. Nanotechnology. 26, 6 (2015). Crossref
10. D. Kuang, L. Xu, L. Liu, W. Hu, Y. Wu. Appl. Surf. Sci. 273, 065706 (2013). Crossref
11. H. Algul, M. Tokur, S. Ozcan, M. Uysal, T. Cetinkaya, H. Akbulut. Applied Surface Science. 359, 484 (2015) . Crossref
12. J. Jiang, X. He, J. Du, X. Pang, H. Yang, Z. Wei. Materials Letters. 220, 178 (2018). Crossref
13. V.G. Konakov, O.Yu. Kurapova, I.V. Lomakin, N.N. Novik, S.N. Sergeev, E.N. Solovyeva, A.P. Zhilyaev, I.Yu. Archakov, I.A. Ovid'ko. Rev. Adv. Mater. Sci. 50, 1 (2017).
14. V.G. Konakov, O.Yu. Kurapova, I.V. Lomakin, I.Yu. Archakov, E.N. Solovyeva, I.A. Ovidko. Rev. Adv. Mater. Sci. 44, 361 (2016).
15. O.Y. Kurapova, A.G. Glukharev, O.V. Glumov, M.Y. Kurapov, E.V. Boltynjuk and V.G. Konakov. Electrochimica Acta. 320 (10), 134573 (2019). Crossref
16. W.S. Hummers Jr., S. William, R.E. Offeman. Journal of the American Chemical Society. 80, 1339 (1958). Crossref
17. S.N. Alam, N. Sharma, L. Kumar. Graphene. 6 (1), 1 (2017). Crossref
18. P. Hidalgo-Manrique, X. Lei, R. Xu, M. Zhou, I.A. Kinloch, R.J. Young. Journal of materials science. 54, 12236 (2019). Crossref